The Shapes of Simple Polyatomic Molecules and Ions. I. The Series HAAH and BAAB

B. M. Gimarc

Contribution from the Department of Chemistry, University of South Carolina, Columbia, South Carolina 29208. *Received June 9, 1969*

Abstract: The general features of the shapes of molecules in the series HAAH and BAAB as determined by extended Hückel calculations are compared with known molecular geometries. Molecular energy levels and simple molecular orbital pictures are presented and used to explain molecular shape as a function of the number of valence electrons in molecules such as C_2N_2, C_2F_2, N_2O_2, N_2F_2, C_2H_2, N_2H_2, and H_2O_2. The mechanism for the *cis–trans* thermal isomerization of N_2H_2 and N_2F_2 is studied. Nonplanar and linear transition states can be ruled out on symmetry or energetic grounds. A planar inversion mechanism is proposed for this process.

The extended Hückel method, developed by Roald Hoffmann,[1] has been used by many investigators to study the geometries of a large number of organic and inorganic molecules. Although exceptions occur, the agreement between the known structures and those calculated by this very crude method should be a source of some satisfaction to theoretical chemists. Most chemists, however, refuse to accept this general agreement between experiment and numerical calculation as an explanation of molecular shapes; they demand a qualitative, pictorial explanation of why the numerical results turn out as they do. This paper describes a simple molecular orbital model, based on the extended Hückel calculations, which explains the main features of shapes of HAAH and BAAB molecules. At the start, it must be emphasized that this model is not necessarily the only one which can furnish a comprehensive explanation of the shapes of these two series. Furthermore, any such model will contain a certain amount of arbitrariness. It is hoped that the model described here relies on at least a smaller number of arbitrary features, and that these will be appropriate for the study of other series of molecules as well.

Mulliken[2] noticed that the shapes of molecules and ions with the general formula AB_2 are determined by the number of valence electrons the molecules contain. Walsh[3] extended these observations to several other series of simple polyatomic molecules; the summaries of these observations are usually called Walsh's rules. Following Mulliken, Walsh discussed the shapes of several different series of simple polyatomic molecules in terms of elementary qualitative molecular orbital theory. He constructed correlation diagrams showing how molecular orbital energy levels change with bond angle. The ordering and slope of the levels were determined in such a way that the results agreed with qualitative reasoning and experimental evidence, such as known molecular shapes and electronic spectra. Walsh's successful explanations of molecular shapes were based on the assumption that all the molecules of a particular series have energy level schemes that are qualitatively similar but differ in the number of occupying valence electrons. It is Walsh's general approach, aided by energy levels and orbitals from extended Hückel calculations, that is used here for the series A_2H_2 and A_2B_2. At best the calculations are only semiquantitative. Therefore, numerical details have been suppressed where possible, in order to reveal more clearly those results of qualitative value. In this paper, orbital pictures and energy level diagrams are presented, together with simple physical rationalizations, which make the shapes of A_2H_2 and A_2B_2 molecules understandable from a molecular orbital point of view. Some simpler series of molecules are described in a similar way by Herzberg.[4] In a less detailed fashion, the shapes of the AB_3 series have been discussed previously.[5]

Table I contains representative A_2H_2 and A_2B_2 molecules of known geometry to be studied in this paper. Many of these interesting molecules were unknown at the time of Walsh's original work. Notice that C_2H_2 (10 valence electrons) is linear, N_2H_2 (12 electrons) has planar *cis* and *trans* conformers,[6] and H_2O_2 (14 electrons) is nonplanar with a dihedral angle ϕ of around 110°.[7] Among the A_2B_2 molecules, those with 22 electrons or less are linear like C_2N_2 and $C_2O_2^{2-}$.[8] Those with 24 electrons are planar, *cis* or *trans*. Both *cis* and *trans* isomers of N_2F_2 exist.[9] Apparently only the *trans*

Table I. A_2H_2 and A_2B_2 Molecules

Valence electrons	Molecule	Structure
10	C_2H_2	Linear, $D_{\infty h}$
12	N_2H_2	Planar *cis* or *trans*; C_{2v} or C_{2h}
14	H_2O_2, H_2S_2	Nonplanar; C_2
18	C_2N_2, B_2O_2	Linear, $D_{\infty h}$
22	C_2F_2, C_2Cl_2, C_2Br_2, $C_2O_2^{2-}$	Linear; $D_{\infty h}$
24	N_2F_2, $N_2O_2^{2-}$	Planar *cis* or *trans*; C_{2v} or C_{2h}
26	O_2F_2, S_2F_2, S_2Cl_2, S_2Br_2	Nonplanar; C_2; dihedral angle = 90°

(1) R. Hoffmann, *J. Chem. Phys.*, **39**, 1397 (1963); **40**, 2047, 2474 (1964); *Tetrahedron*, **22**, 521 (1966).
(2) R. S. Mulliken, *Rev. Mod. Phys.*, **14**, 204 (1942).
(3) A. D. Walsh, *J. Chem. Soc.*, 2260 (1953).
(4) G. Herzberg, "Molecular Spectra and Molecular Structure, III. Electronic Spectra and Electronic Structure of Polyatomic Molecules," D. Van Nostrand Co., Inc., Princeton, N. J., 1965, p 312.
(5) B. M. Gimarc and T. S. Chou, *J. Chem. Phys.*, **49**, 4043 (1968).
(6) K. Rosengren and G. C. Pimentel, *ibid.*, **43**, 507 (1965).
(7) R. H. Hunt, R. A. Leacock, C. W. Peters, and K. T. Hecht, *ibid.*, **42**, 1931 (1965).
(8) E. Weiss and W. Buchner, *Helv. Chim. Acta*, **46**, 1121 (1963).
(9) R. K. Bohn and S. H. Bauer, *Inorg. Chem.*, **6**, 309 (1967).

structure is known for $N_2O_2^{2-}$.[10] A_2B_2 molecules with 26 electrons are skewed and nonplanar. The dihedral angle in O_2F_2, for example, is near 90°.[11] Figure 1 shows how conveniently the different shapes are related to each other.

There are exceptions to the preceding rules. Several alkali metal halides are known to exist in the vapor at high temperatures as diamond-shaped A_2B_2 dimers.[12] Since molecular orbital theory without configuration interaction fails to describe adequately the electronic structure of highly ionic molecules, the alkali halide dimers have been omitted from this study. More serious exceptions to the rules are S_2N_2 and N_2O_2, which surely fall within the province of molecular orbital theory. S_2N_2 (22 electrons) is a ring of alternate S and N atoms,[13] and N_2O_2 (22 electrons) has *cis* and *trans* isomers.[14,15] The empirical parameters for the S and N atoms which serve as input data for the extended Hückel calculations are quite similar. Perhaps S_2N_2 might fit more appropriately into the A_4 series, in which 22-electron rings are known. The N_2O_2 case will be discussed later on in this paper.

In the series of chain-type BAAB molecules, the atoms in the central positions (the A's) have lower electronegativity than the terminal atoms (the B's). There is a qualitative molecular orbital explanation for this. The higher energy molecular orbitals have nodal surfaces that pass through or near the center of the molecule. The nodes reduce the electron density in the center of the molecule and push electron density toward the terminal atoms. The central atoms must be able to give up charge, and the terminal atoms must be able to accept it. In the extended Hückel calculations the valence state ionization potentials are the quantities related to electronegativities.

Calculations

The extended Hückel method is well known, but a minimal discussion of it is necessary here in order to explain some of the details of the models to be presented. The method constructs molecular orbitals for valence electrons only from linear combinations of unhybridized Slater s, p_x, p_y, and p_z valence atomic orbitals, located on nonhydrogen nuclei and parallel to each other in the same arbitrary Cartesian coordinate system; 1s orbitals are centered on the hydrogens. The calculations require the solution of the secular determinant

$$|H_{kl} - \epsilon_j S_{kl}| = 0$$

where the roots ϵ_j are the molecular orbital energies. The total molecular energy E is simply the sum of energies ϵ_j of the individual valence electrons.

$$E = \sum_{\text{valence electrons}} \epsilon_j \qquad (1)$$

The sum E of eq 1 is a very poor approximation to the true molecular energy; but it turns out that for changing bond angles, E quite closely parallels the true molecular energy, as well as the *ab initio* SCF energy, and this

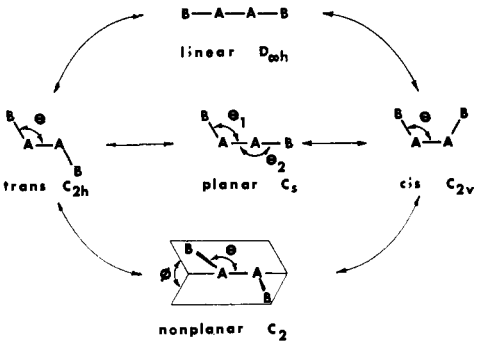

Figure 1. Shapes of A_2H_2 and A_2B_2 molecules.

is responsible for the success of the extended Hückel method in calculating minimum energy geometries. Allen and Russell have discussed this interesting point.[16] The minimum total energy E determines the molecular geometry, but E in turn is determined by the sum of occupied orbital energies ϵ_j. It is the purpose of this paper to examine the individual molecular orbitals in detail and to show qualitatively why the orbital energies produce the molecular shapes they do.

The diagonal matrix elements H_{kk} are approximated by valence state ionization potentials. For studies of molecular shapes, these values need not be chosen with any particular care; there is variety of tabulated values.[17] The off-diagonal elements H_{kl} can be approximated by

$$H_{kl} = 0.5K(H_{kk} + H_{ll})S_{kl} \qquad (2)$$

or

$$H_{kl} = K'S_{kl} \qquad (3)$$

or by similar expressions. Equation 3 works better for A_2H_2 molecules; for the A_2B_2 series eq 2 is satisfactory. N_2H_2 has been studied in detail to get energy levels for a typical A_2H_2 molcule. $K' = -42$ eV gave good results. For the several A_2B_2 molecules investigated, $K = 2.0$ in eq 2 is a reasonable value. The overlap integrals S_{kl} are computed from Slater atomic orbitals. The geometry of the molecule enters the calculation through the overlap integrals, which depend on interatomic distances. From the dependence of H_{kl} on overlap, it follows that if a change in molecular geometry increases the overlap of atomic orbitals in a particular molecular orbital, then that change will stabilize or lower the energy of that molecular orbital. This rule of maximization of overlap is the basis for interpreting qualitatively the changes in the individual energy levels ϵ_j, and hence the total energy E. Another important rule which operates here is the noncrossing rule; *i.e.*, orbitals of the same symmetry cannot cross. The extended Hückel method is known to be poor for minimization of total energy with respect to bond lengths. A quick look at the consequences of eq 2 for the H_2 molecule reveals that the linear dependence of H_{kl} on overlap does not permit an energy minimum anywhere near the observed bond length. Cusachs,[18] using an H_{kl} approximation

(10) J. E. Rauch and J. C. Decius, *Spectrochim. Acta*, **22**, 1963 (1966).
(11) R. H. Jackson, *J. Chem. Soc.*, 4585 (1962).
(12) A. W. Searcy, *Progr. Inorg. Chem.*, **3**, 49 (1962).
(13) J. R. W. Warn and D. Chapman, *Spectrochim. Acta*, **22**, 1371 (1966).
(14) W. G. Fateley, H. A. Bent, and B. Crawford, *J. Chem. Phys.*, **31**, 204 (1959).
(15) W. A. Guillory and C. E. Hunter, *ibid.*, **50**, 3516 (1969).
(16) L. C. Allen and J. D. Russell, *ibid.*, **46**, 1029 (1967).
(17) H. A. Skinner and H. O. Pritchard, *Trans. Faraday Soc.*, **49**, 1254 (1953); H. Basch, A. Viste, and H. B. Gray, *Theor. Chim. Acta*, **3**, 458 (1965); L. C. Cusachs and J. W. Reynolds, *J. Chem. Phys.*, **43**, S160 (1965); L. C. Cusachs, J. W. Reynolds, and D. Barnard, *ibid.*, **44**, 835 (1966); J. Thorhallsson, C. Fisk, and S. Fraga, *Theor. Chim. Acta*, **12**, 80 (1968).
(18) L. C. Cusachs, *J. Chem. Phys.*, **43**, S157 (1965).

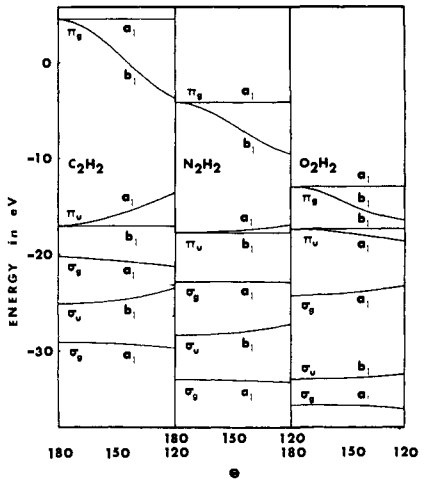

Figure 2. Comparison of extended Hückel orbital energy correlation diagrams for C_2H_2, N_2H_2, and H_2O_2 in *cis* and linear geometries.

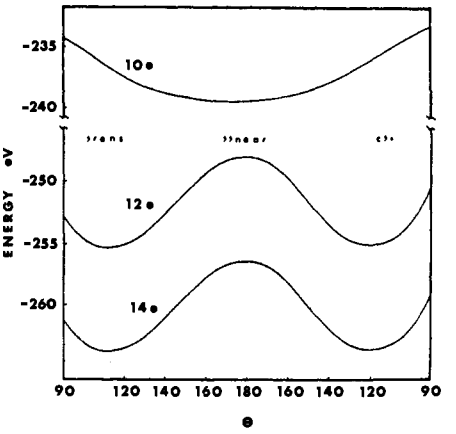

Figure 3. Total energies of the 10-, 12-, and 14-electron systems in the N_2H_2 framework in *cis*, *trans*, and linear shapes.

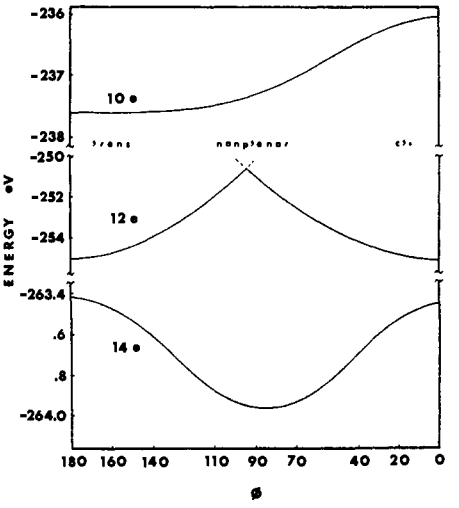

Figure 4. Total energies of the 10-, 12-, and 14-electron systems in the N_2H_2 framework in planar, *cis* and *trans*, and nonplanar shapes.

with a rather more complicated dependence on overlap, has been somewhat more successful with bond length variations. In the calculations required for this paper, bond lengths were kept fixed at experimental values or reasonable estimates, and bond angles were varied to find the geometry with the lowest energy E. A modification of Hoffmann's program, available from the Quantum Chemistry Program Exchange at Indiana University, has been used.

A_2H_2 Molecules

Figure 2 contains portions of the correlation diagrams calculated for C_2H_2, N_2H_2, and O_2H_2. In most respects the diagrams are qualitatively alike. Their differences are easy to understand and, in any case, do not change the conclusions about molecular shape. The decreasing gap between π_g and π_u levels through the series C_2H_2, N_2H_2, O_2H_2 is a consequence of the increasing length of the central A–A bond and the increasing Slater orbital exponent through the series. Later on other differences will be resolved.

N_2H_2 has been studied in detail as the typical A_2H_2 molecule. Alster and Burnelle[19] have done similar calculations for N_2H_2, but the use and interpretation of the results here differ from theirs. For $N_2H_2^{2+}$ (10 valence electrons, isoelectronic with C_2H_2), the minimum energy geometry is linear. The calculations indicate that N_2H_2 is bent with planar *cis* and *trans* conformers. $N_2H_2^{2-}$ (isoelectronic with H_2O_2) has the lowest total energy in the nonplanar, skewed configuration. One should take this last result with some caution. The valence energy level sum, eq 1, formed from the *ab initio* SCF orbital energies, does not pass through a minimum at some intermediate dihedral angle ϕ between *cis* and *trans*. In fact, even the best, properly calculated, *ab initio* SCF total molecular energy does not have a minimum between *cis* and *trans* unless hydrogen p orbitals are included in the basis set, and then the minimum is very shallow and deviates widely from the experimental dihedral angle.[20-22] The problem is a difficult one, because the barriers holding H_2O_2 nonplanar are quite small: 7 and 1 kcal/mole for the *cis* and *trans* barriers, respectively. On the other hand, Gordon and Pople,[23] using the approximate INDO SCF method, do manage to get nonplanar geometry for H_2O_2. For the extended Hückel calculations reported here, the use of eq 3 rather than eq 2 allows one to calculate much deeper H_{kl} elements for the interactions between hydrogen 1s orbitals and A atom p orbitals. These interactions can be viewed as the source of the calculated nonplanar geometry.

Figures 3 and 4 present the total energy E as a function of angles for the 10-, 12-, and 14-electron systems in the N_2H_2 framework. Figure 5 is a correlation diagram, calculated for N_2H_2, showing how molecular orbital energy levels change with symmetric *cis* or *trans* bending, compared to those for linear geometry. In the linear configuration, the σ and π levels in Figure 5 have the same ordering in energy as the *ab initio* SCF levels of C_2H_2 calculated by Buenker, Peyerimhoff, and Whitten.[24] Figure 6 is a correlation diagram for the rotation from planar *trans* to planar *cis* through the nonplanar, skewed configuration of C_2 symmetry. The energy levels in Figure 6 are qualitatively similar

(19) J. Alster and L. A. Burnelle, *J. Amer. Chem. Soc.*, **89**, 1261 (1967).
(20) W. H. Fink and L. C. Allen, *J. Chem. Phys.*, **46**, 2261 (1967).
(21) L. Pedersen and K. Morokuma, *ibid.*, **46**, 3941 (1967).
(22) W. E. Palke and R. M. Pitzer, *ibid.*, **46**, 3948 (1967).
(23) M. S. Gordon and J. A. Pople, *ibid.*, **49**, 4643 (1968).
(24) R. J. Buenker, S. D. Peyerimhoff, and J. L. Whitten, *ibid.*, **46**, 2029 (1967).

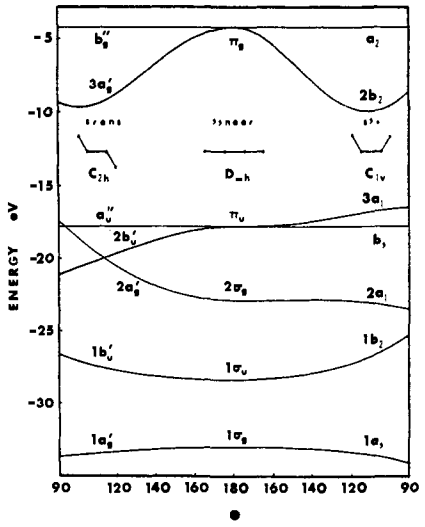

Figure 5. Correlation diagram for N_2H_2 orbital energies in linear, *cis*, and *trans* geometries.

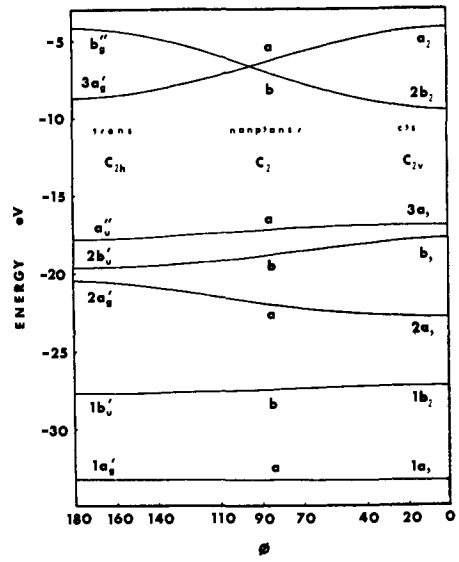

Figure 6. Correlations diagram for N_2H_2 orbital energies in planar, *cis*, and *trans*, and nonplanar geometries.

to the *ab initio* SCF levels calculated for H_2O_2 undergoing this rotation, as reported by Fink and Allen[20] and Palke and Pitzer.[22] Note that the extreme left- and right-hand edges of Figure 6 coincide with the $\theta = 120°$ verticals in the *trans* and *cis* regions of Figure 5.

In the extended Hückel model, an A_2H_2 molecule provides ten atomic orbitals, from which ten molecular orbitals can be constructed. For a linear molecule the molecular orbitals can be divided into two classes: σ orbitals which are cylindrically symmetric about the molecular axis, and π orbitals which are antisymmetric with respect to reflection in a plane containing the molecular axis. Take the molecular axis as the z axis. One can form six σ orbitals from the hydrogen 1s orbitals and the s and p_z orbitals on the A atoms. From the four p_x and p_y orbitals on the A atoms, one can make four π orbitals as two doubly degenerate pairs. On an energy scale, the σ orbitals are the lowest and the highest in energy, with the π orbitals somewhere in between. A reasonable way to divide the two classes energetically is to place three σ levels at low energy, the

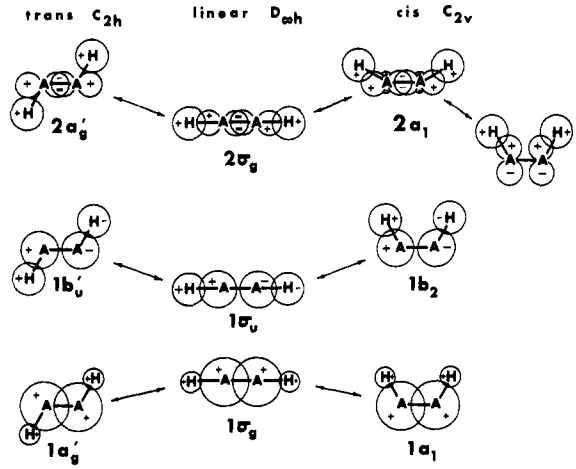

Figure 7. The $1\sigma_g$, $1\sigma_u$, $2\sigma_g$, and related valence orbitals for an A_2H_2 molecule.

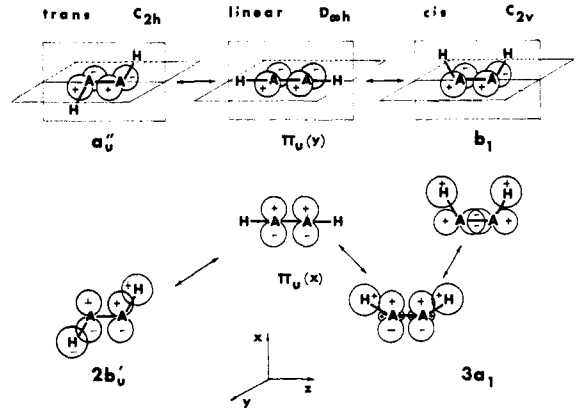

Figure 8. The π_u and related orbitals for A_2H_2.

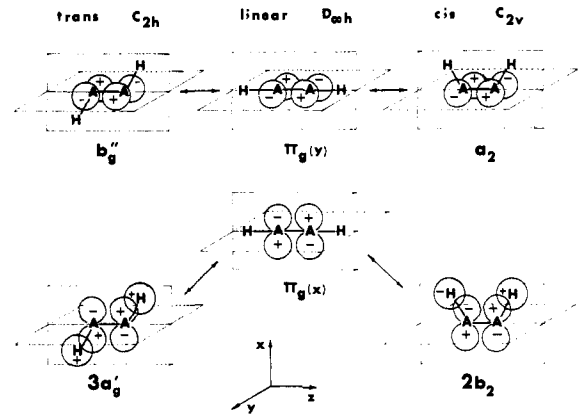

Figure 9. The π_g and related orbitals for A_2H_2.

two doubly degenerate π levels at intermediate energy, and the remaining three σ levels at high energy. These last three high-energy σ levels contain no electrons in the molecules studied here; therefore they have been omitted from the following discussion and all the relevant diagrams.

Figures 7, 8, and 9 show schematically the principal atomic orbitals which make up each of the valence molecular orbitals of a generalized A_2H_2 molecule in linear and bent configurations. Those atomic orbitals which are not major components or are not essential for the

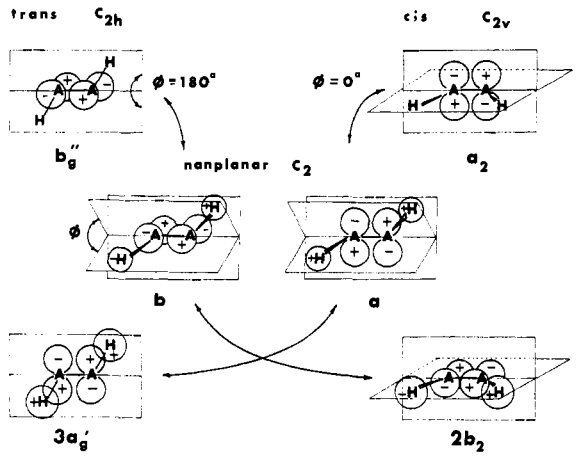

Figure 10. The highest energy a and b orbitals of A_2H_2 under rotation from *trans* to *cis* through nonplanar geometry.

following arguments have been omitted. The lowest energy orbital, $1\sigma_g$, is primarily the sum of the two A atom s atomic orbitals, with very small contributions from the 1s orbitals on the hydrogens. *cis* and *trans* bending in the plane of the page slightly lowers the energy of the $1a_1$ and $1a_g'$ orbitals which stem from $1\sigma_g$, because each hydrogen 1s orbital moves into somewhat better overlap with the s orbital on the opposite A atom. For *cis* geometry the 1s orbitals can overlap rather strongly with each other. The energy lowering compared to $1\sigma_g$ is small because the hydrogen 1s orbitals make such a small contribution to this molecular orbital. Therefore, the $1a_g'$, $1\sigma_g$, $1a_1$ level is the slightly drooping line in the correlation diagram of Figure 5. The next higher orbital, $1\sigma_u$, is mainly the difference between the s orbitals on the two A atoms. $1\sigma_u$ has a nodal plane passing between the two A atoms and perpendicular to the molecular axis. *cis* and *trans* bending of $1\sigma_u$ forces the hydrogen 1s orbitals toward this nodal plane. Since the energy of an electron in an orbital is roughly proportional to the gradient of the orbital, bending increases the gradient and, therefore, the energy of the $1b_2$ and $1b_u'$ levels that come from $1\sigma_u$. The next higher orbital on the energy scale is $2\sigma_g$. This orbital has two nodes and is composed mainly of p_z orbitals pointing toward each other from the A atoms, plus rather sizable contributions from the 1s orbitals on the hydrogens. *cis* or *trans* bending of $2\sigma_g$ pulls the hydrogen 1s orbitals out of overlap with the outer lobes of the p_z orbitals; hence the energy of $2\sigma_g$ should rise on bending. This is true for $2a_g'$, but a complication occurs here for the $2a_1$ level that comes from $2\sigma_g$ in the *cis* conformation. The $2\sigma_g$ level and the π_u level above it are not far apart in energy, and both yield levels of a_1 symmetry in *cis* geometry. On bending, the $2a_1$ level from $2\sigma_g$ should rise in energy, while the $3a_1$ level from $\pi_u(x)$ should fall. The noncrossing rule forbids the intersection of these two a_1 levels, hence their behavior as shown in Figures 7 and 8. Whether $2a_1$ passes through a maximum and $3a_1$ a minimum, as implied in Figures 7 and 8, depends on how close together are π_u and $2\sigma_g$. For C_2H_2, where they are fairly close, the $2a_1$ and $3a_1$ levels diverge on binding. For O_2H_2, where π_u and $2\sigma_g$ are further apart in energy, the *extrema* are present. N_2H_2 is an intermediate case. Figure 2 shows these differences.

The next orbitals on the energy scale are the doubly degenerate π_u pair shown in Figure 8. These orbitals differ from each other only by a 90° rotation about the molecular axis. One can denote them by $\pi_u(x)$ and $\pi_u(y)$, to indicate that they are made up of p_x and p_y orbitals, respectively. Molecular bending removes the degeneracy. For *trans* bending they split into a_u'' and $2b_u'$; for *cis* bending they become $3a_1$ and b_1. In each π_u orbital a nodal plane passes through all four nuclei. These nodal planes prohibit any contribution to π_u from hydrogen 1s atomic orbitals. For *cis* or *trans* bending of $\pi_u(y)$, the hydrogens still lie on the nodal plane (xz, plane of page) and can make no contribution; therefore, the a_u'' and b_1 levels related to $\pi_u(y)$ have the same energy as $\pi_u(y)$. But *cis* or *trans* bending of $\pi_u(x)$ moves the hydrogens away from the nodal surface of this orbital, and they are then able to contribute their 1s orbitals in a bonding way between H and A; each hydrogen 1s orbital can overlap with a lobe of the p_x orbital on the adjacent A atom. Thus, bending should produce $3a_1$ and $2b_u'$ levels of lower energy than $\pi_u(x)$. The $2b_u'$ level is lower, but the $3a_1$ level encounters the noncrossing problem already mentioned. In C_2H_2 (10 electrons) the doubly degenerate π_u levels are the highest energy orbitals filled with electrons. This molecule is linear primarily because of the $1b_u'$, $1\sigma_u$, $1b_2$ level; but $2a_g'$ and $3a_1$ also help out.

A linear N_2H_2 molecule would have each of its π_g levels singly occupied. Bending removes the degeneracy of $\pi_g(x)$ and $\pi_g(y)$. As in the case of $\pi_u(y)$, the levels a_2 and b_g'', which stem from $\pi_g(y)$, are of exactly the same energy as $\pi_g(y)$ itself. The levels $3a_g'$ and $2b_2$, which arise from $\pi_g(x)$ upon *trans* or *cis* bending, are lower in energy because of hydrogen 1s overlap with p_x orbitals on the adjacent A atom. Figure 9 shows the details. It is the energy lowering of the $2b_2$ and $3a_g'$ levels that produces the lower total energies and hence the *cis* and *trans* isomers of N_2H_2.

For O_2H_2 (14 electrons, or the hypothetical ion $N_2H_2^{2-}$), all the levels in Figure 5 are doubly occupied. Clearly, the planar *cis* and *trans* forms must be lower in energy than linear H_2O_2. Now consider the rotation from *trans* to *cis* about the central A–A axis, through the nonplanar, skewed configuration. Figure 6 is the correlation diagram for this process, calculated for the N_2H_2 framework. The most striking feature in this picture is the crossing of the highest filled a and b levels. Figure 10 shows what happens to the $3a_g'$ and b_g'' orbitals of *trans* geometry upon rotation. Consider the *trans* to *cis* rotation taking place with the dihedral angle ϕ diminishing from 180 to 0°, as one might close a book lying open on a desk by lifting both end covers simultaneously. This choice made the results easier to interpret by keeping the C_2 axis fixed during the rotation. The a orbital increases in energy because the hydrogen 1s orbitals are pulled out of overlap with the p_x orbitals on the adjacent A atoms. At $\phi = 0°$ (*cis* geometry), the 1s orbitals disappear entirely from the a orbital because the hydrogens lie on the nodal plane of the p_x orbitals. For a similar reason, the b orbital falls in energy during rotation from *trans* to *cis*, because hydrogen 1s orbitals move into overlapping position with the p_y orbitals on the A atoms. For the a orbital the most favorable position is at $\phi = 180°$, while the b orbital has lowest energy at $\phi = 0°$. The balancing

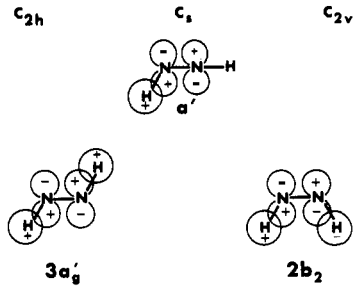

Figure 11. Connection of $3a_g'$ and $2b_2$ orbitals through the C_s planar inversion.

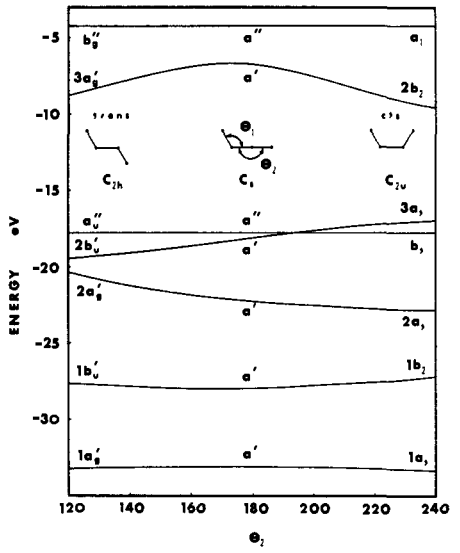

Figure 12. Correlation diagram for N_2H_2 orbital energies in *cis*, *trans*, and C_s geometries.

against each other of the highest filled a and b orbitals is the major factor responsible for the skewed, nonplanar geometry of H_2O_2.

Isomerization of N_2H_2

In their calculations, Alster and Burnelle studied the mechanism and barrier to thermal isomerization of N_2H_2.[19] They considered three possible mechanisms. According to their calculated total energies, the transition state of the highest energy is the linear configuration ($D_{\infty h}$), lower than, that is, the nonplanar, skewed conformation (C_2). The mechanism with the lowest energy transition state is that involving the planar inversion (C_s) in which one HNN angle remains relatively fixed while the opposite hydrogen shifts in the plane from *trans* to *cis*. Refer to Figure 1 for details. Because of the semiquantitative nature of the calculations, consideration of the calculated total energies themselves is not likely to be a reliable way to decide among the possible mechanisms. To gain more insight, look at the changes in the individual orbitals during these processes. In the *trans* isomer of N_2H_2, the highest occupied orbital is $3a_g'$; in the *cis* isomer the highest occupied orbital is $2b_2$. On rotation from *trans* to *cis* through the nonplanar transition state, the *trans* $3a_g'$ orbital moves much higher in energy to become a_2 in *cis* geometry. To avoid moving to this high energy, the electrons would have to cross over to the b orbital which falls during rotation. This, however, would be

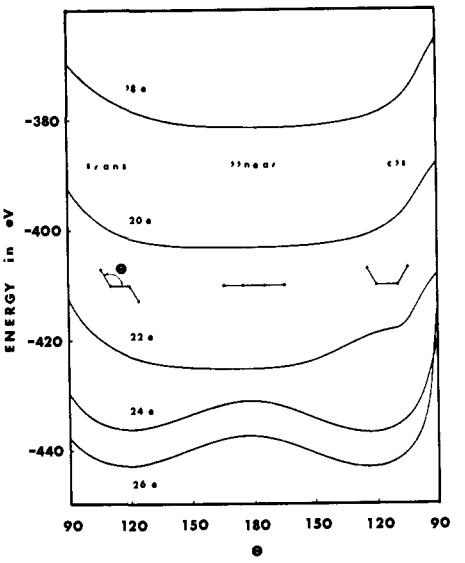

Figure 13. Total energies of the 18-, 20-, 22-, 24-, and 26-electron systems in the $C_2O_2^{2-}$ framework in *cis*, *trans*, and linear shapes.

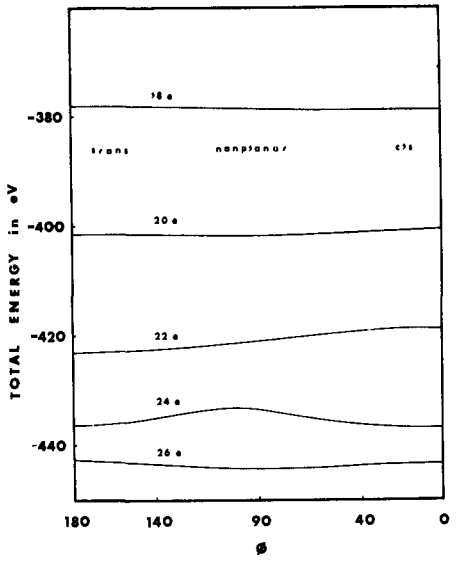

Figure 14. Total energies of the 18-, 20-, 22-, 24-, and 26-electron systems in the $C_2O_2^{2-}$ framework in planar, *cis* and *trans*, and nonplanar shapes.

a violation of the principle of conservation of orbital symmetry, which has been used so successfully by Woodward and Hoffmann to explain the mechanisms of concerted reactions.[25] In the C_s pathway the a,b symmetry is lost and $3a_g'$ can be converted directly to $2b_2$. Figure 11 shows how. It is clear from this picture that a linear transition state would have still higher energy, because hydrogen 1s and p orbitals in both bonding N–H combinations would have to decouple. These arguments strongly favor the planar C_s transition state for the N_2H_2 isomerization. The linear pathway can be ruled out on energetic grounds by qualitative considerations, and the nonplanar rotation is excluded by symmetry conditions. Figures 5 and 6 are correlation

(25) H. C. Longuet-Higgins and E. W. Abrahamson, *J. Amer. Chem. Soc.*, **87**, 2045 (1965); R. Hoffmann and R. B. Woodward, *Accounts Chem. Res.*, 1, 17 (1968); R. Hoffmann, *J. Chem. Phys.*, **49**, 3739 (1968); L. C. Cusachs, M. Krieger, and C. W. McCurdy, *ibid.*, **49**, 3740 (1968).

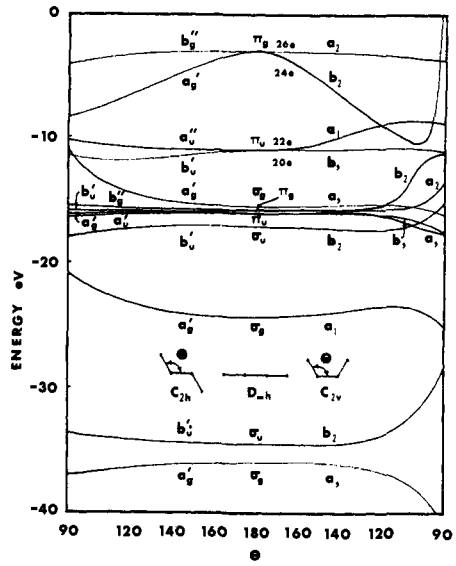

Figure 15. Correlation diagram for $C_2O_2^{2-}$ orbital energies in *cis*, *trans*, and linear conformations.

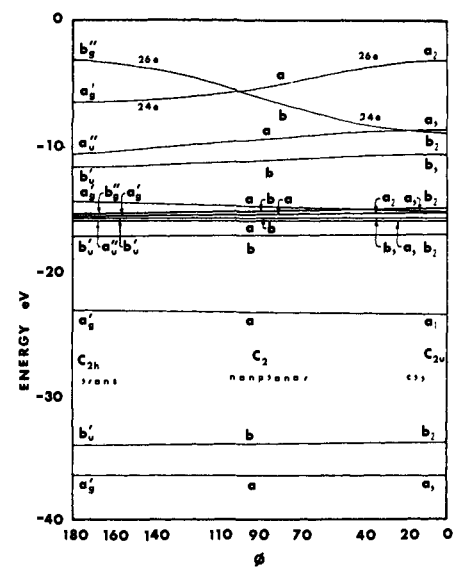

Figure 16. Correlation diagrams for $C_2O_2^{2-}$ orbital energies in planar, *cis* and *trans*, and nonplanar shapes.

diagrams for the linear and nonplanar mechanisms, respectively. Figure 12 is the correlation diagram for the C_s mechanism; notice the hump in the $3a_g'$–$2b_2$ level.

A_2B_2 Molecules

Extended Hückel calculations were performed for C_2N_2, $C_2O_2^{2-}$, N_2O_2, N_2F_2, and O_2F_2. For the following discussion consider the acetylene diolate anion $C_2O_2^{2-}$ (22 valence electrons) as the typical A_2B_2 molecule. Linear shape gives the minimum calculated total energy. Furthermore, the minimum energy geometries of some hypothetical ions are: linear for $C_2O_2^{2+}$ (18 electrons, isoelectronic with C_2N_2), planar *cis* and *trans* isomers for $C_2O_2^{4-}$ (isoelectronic with N_2F_2), and nonplanar with dihedral angle near 90° for $C_2O_2^{6-}$ (isoelectronic with O_2F_2). Figures 13 and 14 present total energy E as a function of angles for the 18-, 20-, 22-, 24-, and 26-electron systems in the $C_2O_2^{2-}$ framework.

The energy levels and molecular orbitals of $C_2O_2^{2-}$ must contain an explanation of the shapes of all the A_2B_2 molecules. On four atoms, each with four atomic orbitals, there are a total of 16 atomic orbitals from which one can form 16 molecular orbitals. For a linear molecule there must be eight σ and eight π molecular orbitals. Figures 15 and 16 are intersecting, valence orbital correlation diagrams calculated for $C_2O_2^{2-}$ showing how energy levels change with changing geometry. These diagrams are a bit more complicated than the corresponding figures for the A_2H_2 series, but they can be interpreted qualitatively in just the same way. Since most of the levels have little effect on molecular geometry, only those which do are discussed. The three molecular orbitals of lowest energy are two σ_g and one σ_u. These are composed primarily of s atomic orbitals, and in many respects are similar to the three low-energy σ orbitals in the linear A_2H_2 system. When filled with electrons, the σ_u and the higher of the two σ_g levels are chiefly responsible for the linear shape of most BAAB molecules with 22 valence electrons or less. Bending BAA angles pushes s atomic orbitals on the terminal atoms toward nodal planes perpendicular to the molecular axis, raising the energy of these levels. For *cis* geometry, both of these σ_g orbitals turn down sharply in energy at around $\theta = 90°$ (rectangular geometry or ring-shaped). These orbitals undoubtedly help make molecules such as S_2N_2 and Se_4^{2+} ring-shaped, but higher energy orbitals probably also assist in these cases. The linear BAAB system contains two sets of doubly degenerate π_u and π_g levels. Of these only the upper π_u and π_g levels are important for molecular geometry. No stable 20-electron BAAB molecules are known. An example would be C_2O_2 which has been proposed as an intermediate in the reaction responsible for ultraviolet chemiluminescence in oxygen–hydrocarbon flames.[26] The extended Hückel calculations and Figure 15 indicate that the C_2O_2 complex should be linear and a diradical, and therefore likely to be highly reactive in any environment in which it might be formed.

For molecules with 24 valence electrons the highest occupied orbitals for linear geometry would be the doubly degenerate upper π_g orbitals, the highest in Figure 15. The upper π_g levels are completely antibonding, composed of p atomic orbitals antiparallel to each other. They can be denoted by $\pi_g(x)$ and $\pi_g(y)$ to indicate that they are made up of p_x or p_y atomic orbitals. For a linear 24-electron molecule, each upper π_g level would contain a single electron only. Bending removes the degeneracy of $\pi_g(x)$ and $\pi_g(y)$. For *cis* bending the two levels become a_2 and b_2; for *trans* bending they become b_g'' and a_g'. Figure 17 shows the changes in the upper π_g orbitals due to bending in the xz plane. Once the molecule is bent and a nodal surface no longer passes through the terminal (B) nuclei, the orbitals a_2, b_2, b_g'', and a_g' can contain p_z and s atomic orbitals as well as p_x or p_y. The p_z and s contributions are not small, but for simplicity the molecular orbital pictures presented here contain only the p_x or p_y atomic orbitals. With *cis* bending the energy of the b_2 level drops well below that of the linear $\pi_g(x)$, because the lower lobes of the B atom p_x atomic orbitals move from antibonding positions into favorable bonding positions, with respect to the neighboring A atom

(26) K. D. Bayes, *Bull. Am. Phys. Soc.*, 13, 374 (1963).

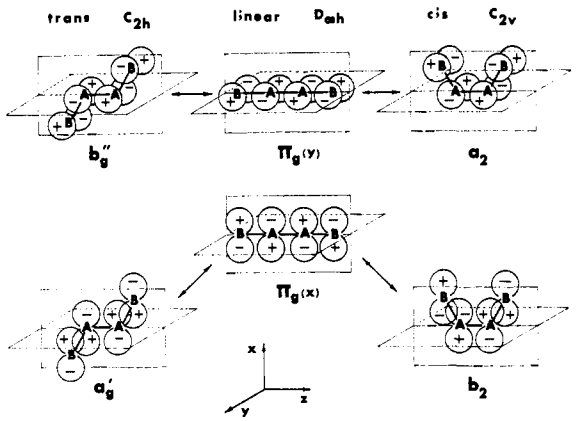

Figure 17. The upper π_g and related orbitals for A_2B_2.

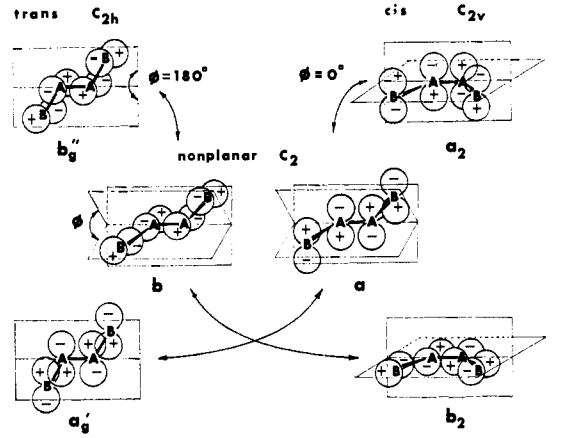

Figure 18. The highest a and b orbitals of A_2B_2 under rotation from *trans* to *cis* through nonplanar geometry.

p_x orbitals. Notice that in this model the p orbitals move with the atoms but remain locked parallel to the coordinate axis; this is consistent with the way the extended Hückel calculations are carried out. In *cis* geometry the energy of a_2 changes very little from that of $\pi_g(y)$; no new overlaps come into play. For *trans* bending the p_x orbitals on the B atoms move into bonding positions with respect to their neighboring A atoms; therefore, the a_g' level should be lower in energy than $\pi_g(x)$. Again there should be little change in b_g'' compared to $\pi_g(y)$. It is the b_2 (*cis*) and a_g' (*trans*) energy levels which give *cis* and *trans* shapes to 24-electron BAAB molecules.

For a 26-electron molecule all the levels shown in Figure 15 would be doubly occupied. Clearly the planar *cis* and *trans* forms would be lower in energy than a linear arrangement. Now imagine rotating the end B atoms about the A–A axis from *trans* to *cis* through the nonplanar C_2 shape. Figure 18 shows what happens to the highest a_g' and b_g'' orbitals upon rotation. The p orbitals continue to point along the fixed coordinate axes. In rotating from *trans* to *cis*, the b_g'' level drops in energy to become b_2, because rotation allows the p_y orbitals on the B atoms to move from antibonding positions in b_g'' into bonding positions in b_2, with respect to the p_y orbitals on the adjacent A atoms. The a_g' level rises in energy during *trans* to *cis* rotation to become a_2 because this motion pulls lobes of p_x orbitals on the B atoms out of bonding position and makes an antibonding a_2 arrangement. For the b orbital the dihedral angle for lowest energy is $\phi = 0°$; for the a orbital the best angle is $\phi = 180°$. The balancing against each other of the highest filled a and b orbitals at an intermediate dihedral angle is clearly the major factor responsible for the skewed, nonplanar geometry of 26-electron BAAB molecules. The sum of these a and b levels in $C_2O_2^{6-}$ does not, however, pass through a minimum between $\phi = 180$ and 0°. The minimum total energy at around 90° calculated for $C_2O_2^{6-}$ actually results from a delicate balance among the four highest levels in Figure 16.

This model may account for the shapes of some 26-electron molecules, but it may not hold for O_2F_2. While the extended Hückel correlation diagrams for molecules like C_2N_2 and N_2F_2 are in most respects qualitatively similar to Figures 15 and 16, the O_2F_2 correlation diagrams show a different ordering of energy levels. To understand these differences, consider the energy

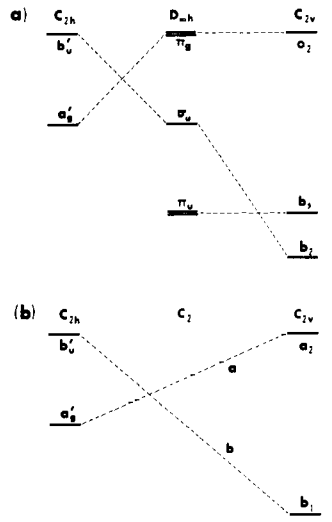

Figure 19. Schematic diagram of highest filled levels of O_2F_2. (a) Relationship between linear and planar, *cis* and *trans*, levels. (b) Rotation from *trans* to *cis* through nonplanar geometry.

levels O_2F_2 would have if it were linear. For linear molecules, σ orbitals can contain only s and p_z atomic orbitals, and π orbitals are composed of either p_x or p_y orbitals only. The valence state ionization potentials ($-H_{kk}$) of all atomic orbitals increase from left to right across a row in the periodic table, but the values for the s orbitals increase more than those for p orbitals. This means that while the π levels of linear O_2F_2 are somewhat lower in energy than those for $C_2O_2^{2-}$ (shown in Figure 15), the σ levels of O_2F_2 will be much lower relative to the π levels, and some interchanges in order or inversions occur.

For the shape of O_2F_2 the most important of these interchanges involves the upper π_g levels and the σ_u level which lies above π_g in the $C_2O_2^{2-}$ system (this σ_u level is positive and not shown in Figure 15), but which is below the upper π_g levels in the energy diagram for O_2F_2. Only the highest occupied levels of this system are shown, schematically, in Figure 19a. For 26 electrons and a linear arrangement, this σ_u level is filled, and each of the degenerate π_g levels above it are singly occupied. Bending, *cis* or *trans*, removes the degeneracy as before. For *trans* bending it is the a_g' level which arises directly from $\pi_g(x)$ that is responsible

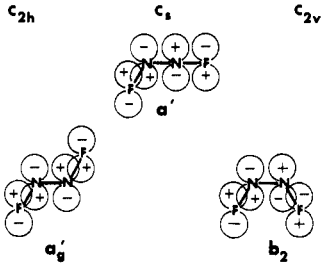

Figure 20. Connection between highest filled a_g' and b_2 orbitals through the planar C_s inversion.

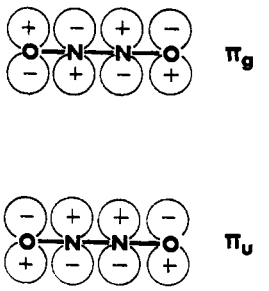

Figure 21. The upper π_g and π_u levels of N_2O_2.

for energy lowering, as shown in Figure 17. For *cis* bending, however, the b_2 level which stabilizes the *cis* structure relative to the linear arrangement is not connected to $\pi_g(x)$, but stems from the σ_u level below it. Symmetry requires that both σ_u and one member of the π_g pair become b_2 on *cis* (C_{2v}) bending. Bending of a high-energy σ_u level, with its many nodal surfaces perpendicular to the molecular axis, should turn it into a b_2 level of higher energy. Bending of the $\pi_g(x)$ level should produce a b_2 orbital of lower energy as in Figure 17. That these two b_2 orbitals should cross is forbidden by the noncrossing rule. Therefore, the b_2 level of the type shown in Figure 17 is actually connected to σ_u rather than $\pi_g(x)$.

Now consider the rotation from *trans* to *cis* through nonplanar C_2 geometry. Figure 19b shows schematically how the highest occupied levels change upon rotation. These are the only levels that change much during rotation; the others change hardly at all. The balancing of these a and b levels against each other does account quantitatively for most of the energy stabilization of O_2F_2 in nonplanar C_2 geometry. The a_2 and a_g' levels are related as shown in Figure 18. The connection between b_2 and b_u' cannot be made so pictorially. A relationship exists to the b_2–b_g'' connection in Figure 18. In O_2F_2, the interposition of a σ_u level, which forms b_u' and b_2 levels on bending, inserts a b_u' level below b_g''. The noncrossing rule blocks the connection between b_2 and b_g'' of Figure 18.

Barriers to Isomerization and Rotation

Binenboym and coworkers[27] found the activation barrier for *trans* to *cis* thermal isomerization of N_2F_2 to be about 32 kcal/mole. Three mechanisms, involving linear $D_{\infty h}$, nonlinear C_s, and nonplanar C_2 transition states, have been considered for the isomerization. Both extended Hückel and CNDO molecular orbital methods have been used to study these mechanisms.[28–30] The results of various investigators all agree that the linear transition state is of very high energy (around 100 kcal/mole), but the planar C_s and nonplanar C_2 transition states are of comparable calculated energy and are, in any case, much larger than the experimental activation energy by about a factor of 2. The calculated total energies of the transiton states tell only part of the story, however. The *trans* to *cis* rotation of N_2F_2 through the nonplanar C_2 transition state involves the crossing of highest filled and lowest empty a and b orbitals. Refer to Figures 16 and 18, keeping in mind that in those pictures the highest energy orbitals, a_2 and b_g'', are vacant for N_2F_2. The problem is very much like that in the N_2H_2 isomerization. The principle of conservation of orbital symmetry, therefore, rules out the C_2 mechanism. In the C_s pathway the highest filled a_g' orbital can convert into b_2 because a,b symmetry is lost. Figure 20 contains a pleasing model for this. The picture also shows why the linear transition state should have still higher energy. Actually, an energy level crossing flaws the simple model of Figure 20. The highest energy b_2 level in Figure 15 lies just below the a_1 level at the minimum total energy bond angle. On inversion the a_g' level connects with a_1, not b_2. While Figure 15 was constructed from results calculated for $C_2O_2^{2-}$, the comparable diagram for N_2F_2 shows the same behavior. The conclusions, however, remain unchanged: the mechanism involving rotation about the N–N bond is forbidden by symmetry, and simple energetics favor the planar inversion mechanism over that involving the linear transition state.

N_2O_2

Although nitric oxide, NO, shows little tendency to dimerize in the gas phase, evidence for the existence of some gas phase dimer $(NO)_2$ has been observed in a variety of experiments.[31] The infrared spectrum of matrix-isolated $(NO)_2$ has been studied by Fateley, Bent, and Crawford,[14] and more recently by Guillory and Hunter.[15] Their results indicate *cis* and *trans* isomers of N_2O_2. The isoelectronic species C_2F_2 and $C_2O_2^{2-}$ are linear. The correlation diagram, Figure 15, suggests how *cis* and *trans* isomers might be possible for the 22-electron molecule. If the upper π_g and π_u levels were closer together, the a_g' and b_2 levels, which split from π_g when the molecule is bent, could dip below the a_u'', b_u' or a_1, b_1 levels related to π_u. Figure 21 shows the upper π_g and π_u levels. Notice that π_u is bonding between the two N atoms, while π_g is antibonding. Lengthening the central bond would make π_u go higher in energy, because it would be pulling apart two bonding fragments; and it would make π_g lower, since it would separate two nonbonding parts. Now, N_2O_2 is a very weak dimer, and one would expect the central N–N bond to be long as well as weak. The N–N bond in the stronger dimer N_2O_4 is 1.75 Å long. Assuming this value in an extended Hückel calculation does in fact force π_g and π_u close enough together to produce

(27) J. Binenboym, A. Burcat, A. Lifshitz, and J. Shamir, *J. Amer. Chem. Soc.*, **88**, 5039 (1966).
(28) W. C. Herndon, J. Feuer, and L. H. Hall, *Theor. Chim. Acta*, 11, 178 (1968).
(29) M. S. Gordon and H. Fischer, *J. Amer. Chem. Soc.*, **90**, 2471 (1968).
(30) N. K. Ray and P. T. Narasimhan, *Theor. Chim. Acta*, **9**, 268 (1968).
(31) R. L. Scott, *Mol. Phys.*, 11, 399 (1966); D. Golomb and R. E. Good, *J. Chem. Phys.*, **49**, 4176 (1968).

cis and *trans* configurations for this 22-electron molecule.

An interesting result of the N_2O_2 calculation is the geometry of the $N_2O_2^{4-}$ ion. This would be isoelectronic with Cl_2O_2, another loose dimer, recently detected by matrix-isolation techniques by Pimentel and coworkers.[32] The calculations suggest that the $N_2O_2^{4-}$ ion should be bent, but with completely free rotation about the central bond.

(32) M. M. Rochkind and G. C. Pimentel, *J. Chem. Phys.*, **46**, 4481 (1967); W. G. Alcock and G. C. Pimentel, *ibid.*, **48**, 2373 (1968).

Conclusion

A combination of semiquantitative calculations and qualitative molecular orbital reasoning can provide simple pictorial explanations for the shapes of polyatomic molecules. Where symmetry helps out, one can also get an understanding of isomerization processes. Many other interesting series of related molecules remain to be studied in a similar way.

Acknowledgment. I gratefully acknowledge the generous amount of computer time made available by the Computer Center of the University of South Carolina.

The Interaction of Oxygen with Organic Molecules. I. Absorption Spectra Caused by Adsorbed Organic Molecules and Oxygen

H. Ishida, H. Takahashi, H. Sato, and H. Tsubomura

Contribution from Department of Chemistry, Faculty of Engineering Science, Osaka University, Toyonaka, Osaka, Japan. *Received June 30, 1969*

Abstract: Electronic absorption spectra, arising from interactions between oxygen and aromatic compounds adsorbed on porous glass or silica gel, were measured. Unlike the spectra induced by oxygen in organic solvents, absorption spectra with a certain number of clear maxima have been observed in most cases. These maxima have been interpreted to represent separate charge-transfer excited states, of which the theoretical aspects are discussed. The effect on the spectra of lowering the temperature has been studied. Strong adsorption spectra caused by the singlet → triplet transitions have been obtained for naphthalene adsorbed on porous glass immersed in liquid oxygen. Charge-transfer absorption spectra arising from the interaction between iodine and aniline derivatives adsorbed on silica gel have also been measured, and the results are discussed in relation to the oxygen–aniline systems.

Evans found that oxygen dissolved in aromatic solvents gives rise to extra absorption bands at wavelengths longer than the absorption edges of the aromatics.[1a] Many experiments related to this problem have been done, and now it seems to be quite reasonable that the extra absorption bands are caused by the charge-transfer interaction between oxygen, as an electron acceptor, and organic molecules, as electron donors, although no stable complexes are formed between them.[1c,2-5] Therefore, these absorption bands can be considered to be quite similar to the contact charge-transfer bands found in iodine solutions.[6,7] Evans[1b] also found additional small peaks at the long-wavelength tail of the extra absorption bands when oxygen is dissolved under high pressure in the solutions of aromatic compounds, or when it is mixed with aromatic vapor. He concluded that these weak bands are singlet–triplet absorption bands enhanced by oxygen. Theoretical investigations of these phenomena were also undertaken by many authors.[3,8,9] The contribution of the charge-transfer state in which an electron is removed from the donor molecule to the oxygen molecule has been pointed out. However, the relative importance of the charge-transfer or the exchange mechanism in perturbing the singlet–triplet transition is still open to question, though it would depend on the system, as well as on the orientation of one molecule to another. No detailed information on the electronic energy levels of the charge-transfer states has been obtained, since the extra absorption bands found so far in solutions show no absorption maxima but increase monotonically toward shorter wavelength.

It was expected that the technique of adsorption would afford new means for understanding the nature of intermolecular interaction.[10-12] In the present work, the measurement and interpretation of the absorption spectra caused by the interaction between oxygen and organic molecules adsorbed on the solid surface are carried out. Moreover, the characteristics of intermolecular interaction in the adsorbed state, as well

(1) (a) D. F. Evans, *J. Chem. Soc.*, 345 (1953); (b) *ibid.*, 1351, 3885 (1957); 2753 (1959); 1735 (1960); (c) *ibid.*, 1987 (1961).
(2) A. U. Munck and J. R. Scott, *Nature*, 177, 587 (1956).
(3) H. Tsubomura and R. S. Mulliken, *J. Am. Chem. Soc.*, **82**, 5966 (1960).
(4) J. Jortner and U. Sokolov, *J. Phys. Chem.*, **65**, 1633 (1961); L. Paoloni and M. Cignitti, *Sci. Rept. Ist. Super. Sanita*, **2**, 45 (1962).
(5) E. C. Lim and V. L. Kowalski, *J. Chem. Phys.*, **36**, 1729 (1962); H. Bradley and A. D. King, *ibid.*, **47**, 1189 (1967).
(6) L. E. Orgel and R. S. Mulliken, *J. Am. Chem. Soc.*, **79**, 4839 (1957).
(7) D. F. Evans, *J. Chem. Phys.*, **23**, 1426 (1955).
(8) G. J. Hoijtink, *Mol. Phys.*, **3**, 67 (1906).
(9) J. N. Murrel, *ibid.*, **3**, 319 (1960).
(10) A. D. McLachlan, *ibid.*, **7**, 381 (1964).
(11) H. Sato, K. Hirota, and S. Nagakura, *Bull. Chem. Soc. Jap.*, **38**, 962 (1965).
(12) N. Okuda, *J. Chem. Soc. Jap., Pure Chem. Sect.*, **82**, 1118 (1961).